Modeling of analog optical fiber link with highly nonlinear Mach-Zehnder modulator

Antonio Alves Ferreira Júnior[1], José Antônio Justino Ribeiro[1], and José Edimar Barbosa Oliveira[2]
[1]Instituto Nacional de Telecomunicações – INATEL, Avenida João de Camargo, 510, Santa Rita do Sapucaí, 37540-000, MG, Brasil
[2]Instituto Tecnológico de Aeronáutica – ITA, Praça Marechal Eduardo Gomes, 50, São José dos Campos, 12228-900, SP, Brasil

***Abstract* — This paper addresses the subject of optical fiber chromatic dispersion effect on the performance of an analog optical link using a highly nonlinear dual-drive electro-optic Mach-Zehnder modulator. A direct detection link model which emphasizes the modulator electronic drive, the dispersion characteristic of a linear optical fiber, and the modulator nonlinearities, is discussed. A frequency domain analytical model which yields a rather insightful large-signal analysis of the link performance for either double or single sideband analog optical modulation formats is presented. The model is illustrated by predicting the dependence of the performance of an optical fiber link with respect to the link length, and also shows the influence of the large modulation index value. Some preliminary results of numerical simulations for a link that comprises optoelectronic components for practical applications were also provided.**

***Keywords* — Analog optical fiber link, nonlinear dual-drive Mach-Zehnder modulator, optical fiber chromatic dispersion.**

I. INTRODUCTION

Due to the evidence that the microwave photonic technology will be playing a major role in global interconnectivity, many efforts have been direct toward researches and development on the field of optical fiber link. The microwave photonics technology focuses on generation, processing, control and transmission of radio-frequency (RF) signals by using photonic devices. A great deal of emphasis continues to be driven by military and commercial demands, which aim at performance on the subjects of photonic generation and processing of RF signals, microwave photonic filters, radio-over-fiber (RoF), antenna-remoting and beamforming, and so on [1]-[8].

The broadband and low loss offered by optical fiber communication led to interest in implementation and design of photonic assisted solutions for long-haul high-capacity communications systems. The majority of worldwide communications services as voice, data, video, and advanced internet applications are transported using optical fibers, forming an interconnected global optical network. The desire for high-capacity transported per fiber and low cost per information transmitted led to researches in optically networks with high spectral efficiencies. The demand for high-capacity and wide bandwidth increases at about 60% per year. Advanced optical modulation formats have become the key to the design of modern optical fiber communication systems [9]-[11].

A. A. Ferreira Júnior, antonioa@inatel.br; J. A. J. Ribeiro, justino@inatel.br; J. E. B. Oliveira, edimar@ita.br

Analog photonic links have attracted significant interest in many applications, such as phased-array antennas, radar systems, wireless communications RoF access, broadband cable-television networks, electronic warfare, RF up-conversion, etc. [12]-[20]. Nowadays, the use of large value of modulation index became attractive in instrumentation and waveform generation applications. The high-frequency characterization and the measure of modulation efficiency of an optical modulator have been proposed [21]. A high resolution and wideband optical vector network analyzer was demonstrated with single and double sideband optical modulators [22]-[23]. A triangular pulse generator was proposed based on photonic-assisted devices [24].

This paper is concerned with the effect of a highly nonlinear electro-optic modulator on the performance of an analog optical link by using a linear and dispersive optical fiber. An intensity modulation and direct detection (IM-DD) link model which emphasizes the external modulator electronic drive, the effect of dispersion characteristic of a standard single-mode linear optical fiber (SSMF), and the modulator nonlinearities, is discussed. The model enable the influence analysis for large values of RF modulation index, permits one to quickly retrieve a wide range of known results available on a rather ample literature, and reduced numerical simulation time. A frequency domain analytical model approach which yields a rather insightful analysis of the link performance is presented. The model is illustrated by predicting the dependence of the performance of an optical fiber link with respect to the link length. Some preliminary numerical simulations for a link which comprises optoelectronic components for practical application are given.

This publication consists of four other sections. The statement of the problem, which comprises an overview of the optical link components, is given in the Section II. An analytical frequency domain model for a single RF tone analog fiber link is discussed in Section III. Numerical simulated results are presented and discussed in Section IV, and a few conclusions are presented in Section V.

II. STATEMENT OF THE PROBLEM

A simple block diagram of an optical fiber link is shown in Fig. 1, where different types of optical and optoelectronic components can be used to implement a modern optical fiber system [25]. The electrical signal is converted to optical signal (E/O conversion) by using direct or external modulation processes, and will be transported over the fiber link. At the receiver, a photodiode is used to convert the optical signal to electrical signal (O/E conversion). It should be pointed out that the optical intensity modulator and the square-law photodetector are nonlinear devices, in which introduce RF distortions into the system. Also, the effect of fiber chromatic dispersion will limit the transmission distance in a long-haul optical link, as well the optical signal may experience fiber nonlinearities if the optical power is large to excite the nonlinear fiber effects. So, it is important to mitigate these impairments to improve the signal quality and system performance [26].

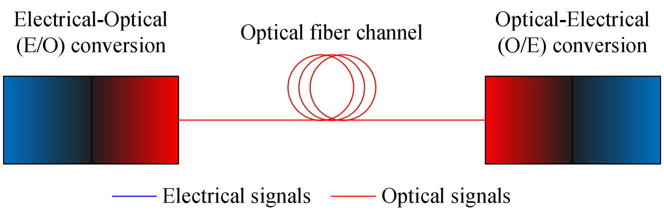

Fig. 1. A simple block diagram of an optical fiber link.

This paper is focused on a typical schematic representation of the IM-DD link with a transmitter, an optical channel, and a receiver, as illustrated in Fig. 2(a). At the input side, a continuous wave from a distributed feedback single-mode laser diode (DFB-LD) generates a carrier at a desired optical wavelength, and a dual-drive integrated electro-optic Mach-Zehnder modulator (DD-MZM) imposes an analog RF signal on the optical carrier. This signal is applied to an optical fiber link and at its output a photodetector (PD) is employed to recover the analog RF signal from its optical carrier. In Fig. 2(b), the external electro-optic modulator electronic driver is emphasized. It is worthwhile to point out that the DD-MZM plays an important role in the link for it enables the wideband implementation of single (OSSB) and double sideband (ODSB) analog optical modulation formats. A great deal of such control may be achieved through the electronic driver, by choosing the phase shift (θ_1) and the bias (θ_2) of the applied electrical signals to the modulator electrodes.

Assuming a balanced splitting ratio of the DD-MZM Y-junctions, a rigorous analysis of the chromatic dispersion effect on the performance of an analog link was provided by [27], with expressions in an infinite series formats. Such drawback is overcome by means of an analytical model in closed-form expressions for the power at the PD output [28]. In these works, the small-signal condition was considered, i.e., small modulation index value.

A DFB-LD generates an optical carrier at a desired wavelength/frequency with a complex output optical field given by [29]

$$E_o(t) = \sqrt{2\xi P_o(t)}\, e^{j[\omega_o t + \phi_o]} \tag{1}$$

where ω_o is the mean optical frequency, ϕ_o is an arbitrary initial optical phase, $P_o(t)$ is the optical power, and ξ (Ω/m^2) is a constant that depends on both the laser beam effective cross-section and the optical wave impedance. The present publication relies on the often used approach in the analysis of IM-DD optical links according to which the laser average power and its phase are time invariant [27],[28].

In Fig. 2(b) one should observe that the optical power delivered by the laser diode reaches the input Y-junction of the integrated z-cut $LiNbO_3$ DD-MZM. Then, it is divided into two parts according to a splitting ratio, determined by the Y-junction power transmission coefficient (r_1) [30]. The simplified view of an integrated DD-MZM is illustrated in Fig. 3, where (a) shows the top view in which the optical waveguides are properly positioned with respect to the RF modulation field pattern, and (b) shows the cross-section view [31],[32].

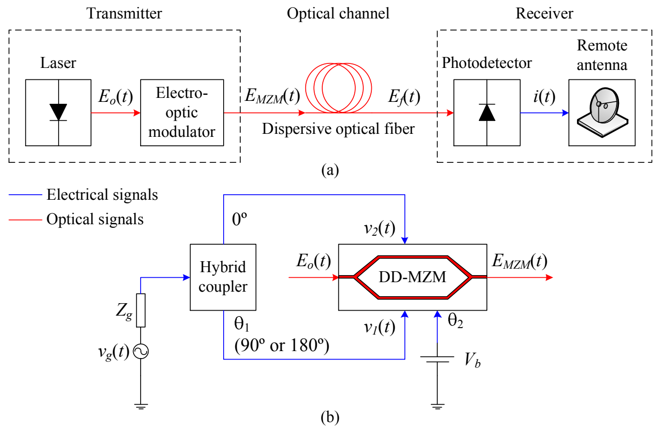

Fig. 2. Overall architecture of the IM-DD analog optical fiber link, where (a) shows the transmitter, optical channel and receiver, and (b) presents the DD-MZM electronic driver.

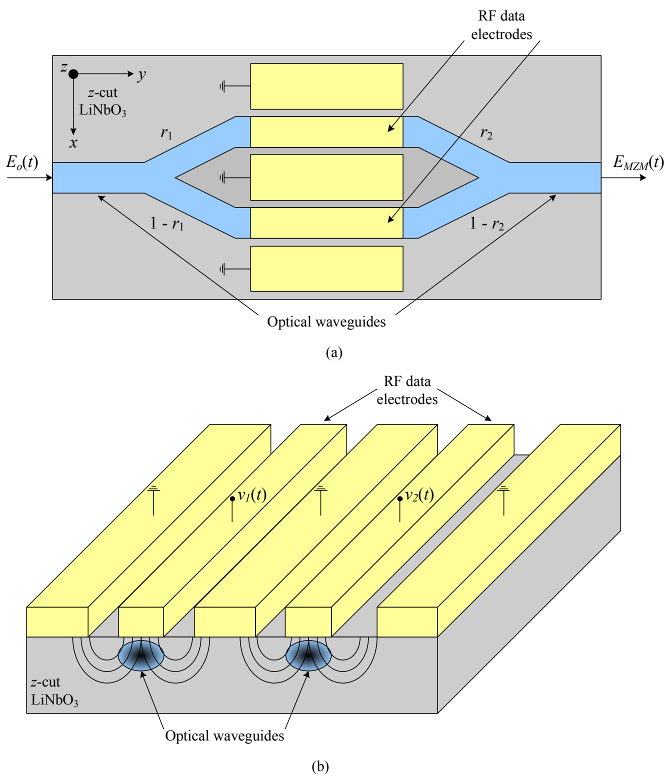

Fig. 3. Simplified integrated DD-MZM with a z-cut $LiNbO_3$ substrate using an optical TM mode, where (a) is the top view showing the Y-junctions transmission coefficients, and (b) shows the cross-section view.

After a MZM's configuration is specified, its performance dependence on substrate orientation and electrodes geometry can be predicted through the variation of the optical phase factor by using a standard perturbation analysis. As a consequence of the electro-optic effect, a RF signal can be used to control the phase of the optical field associated with each optical power parcels as they propagates through the distinct arms of the DD-MZM. It is worthwhile to point out that in the configuration selected in Fig. 3 the optical guided mode has transverse magnetic (TM) polarization, since it enables the utilization of the strongest $LiNbO_3$ electro-optic coefficient (r_{33}). The RF signal, henceforth named modulation signal, must generate an electric field having both a temporal and a spatial pattern adequately distribute in order to reach some key requirements performance, such as low RF power consumption and wide RF bandwidth [33],[34].

The optical phase variations introduced in the arms of the DD-MZM through linear electro-optic effect are given by

$$\phi_1(t) = \frac{\pi}{V_\pi} v_1(t) = m_1 \cos(\omega_{RF} t + \theta_1) \tag{2.a}$$

$$\phi_2(t) = \frac{\pi}{V_\pi} v_2(t) = m_2 \cos(\omega_{RF} t) \tag{2.b}$$

$$\phi_b = \frac{\pi}{V_\pi} V_b = \theta_2 \tag{2.c}$$

where $v_1(t)$ and $v_2(t)$ are instantaneous values of the modulating signals applied to the lower and upper electrodes of DD-MZM, ω_{RF} is the angular frequency of the RF signal, θ_1 is the phase difference between the signals, θ_2 is the phase variation due to the voltage bias (V_b) applied to the proper access, and V_π is the DD-MZM half-wave switching voltage. The coefficients m_1 and m_2 are the modulation indexes due to their signals in the lower and upper arms. They are given, respectively, by

$$m_1 = \frac{\pi V_1}{V_\pi} \tag{3.a}$$

$$m_2 = \frac{\pi V_2}{V_\pi} \tag{3.b}$$

where V_1 and V_2 are the amplitudes of RF signals in lower and upper arms of DD-MZM. It can be shown that the optical electrical field at the output of the DD-MZM has the following complex form, taking into account the output Y-junction power transmission coefficient (r_2) and based on it having a 50/50 splitting ratio

$$E_{MZM}(t) = \frac{E_o}{2} e^{j\omega_o t} \sum_{n=-\infty}^{+\infty} a_n e^{jn\omega_{RF} t} \tag{4}$$

where

$$a_n = j^n \left[J_n(m_1) e^{j(n\theta_1 + \theta_2)} + J_n(m_2) \right] \tag{5}$$

$E_o = \sqrt{(2\xi P_o)}$, and $J_n(.)$ is the first kind Bessel's function with order n. It should be pointed out that (4) applies to DD-MZM with arbitrary modulation signals. It is readily seen that the optical field at the DD-MZM output indeed consists of an infinite series of optical spectral components, i.e., an optical carrier component at ω_o, and an infinite number of sidebands with frequencies $\omega = \omega_o + n\omega_{RF}$ and amplitude a_n.

A small-signal analysis which enables one to identify the requirement that should be satisfied by the DD-MZM drive electronics in order to obtain specific analog optical modulation formats was performed in [35]. For example, OSSB and ODSB can be obtained when the pair of parameters (θ_1,θ_2) obeys the following constraint ($\pi/2$,$\pi/2$) and (π,$\pi/2$), respectively. The DD-MZM output spectrums for the ODSB and OSSB situations are illustrated in Fig. 4, with the RF harmonic order (n) varying from –3 to +3. In Fig. 4(a), all these sidebands are presented and this case refers to ODSB modulation. In Fig. 4(b), we observe that the ideal OSSB modulation is achieve if the modulation index is low, i.e., in the small-signal condition. In this illustration, there are presented the ±2 and +3 sidebands beyond the fundamental component (–1), which can introduce measurement error in the detected signal at PD due to the spectral components beat by the –2 and –1, +2 and +3. As the larger the modulation index is, the measurement error increases [36].

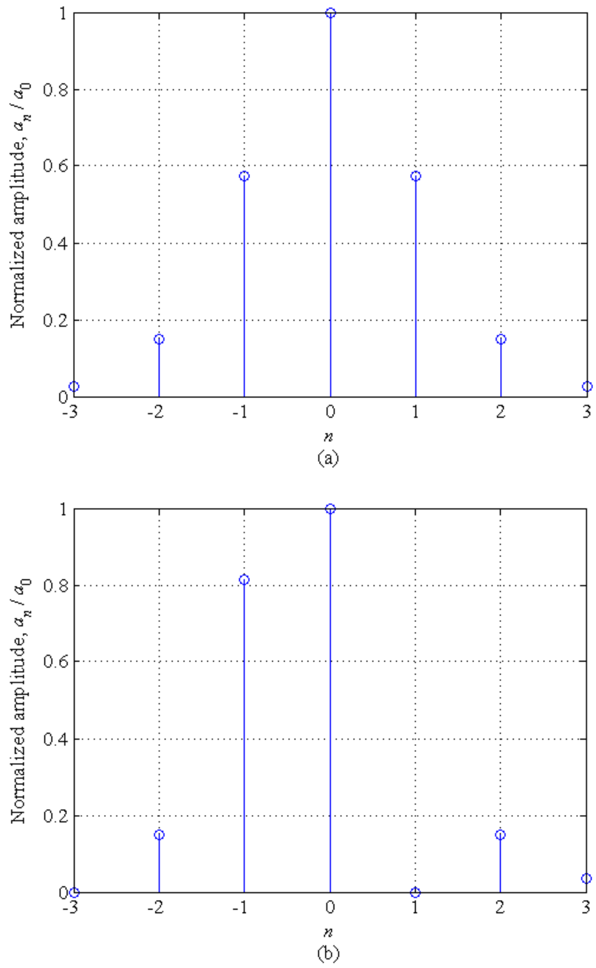

Fig. 4. The DD-MZM output spectrums for the (a) ODSB (π,$\pi/2$) and (b) OSSB ($\pi/2$,$\pi/2$) analog optical modulations, where the RF harmonic order n varies from –3 to +3.

The optical signal at the output of the modulator feeds a spool of a linear SSMF. For instance, in the fiber modeling, a fused silica glass SSMF operating at 1550nm wavelength is considered to be linear with constant loss $\alpha(\omega)$ (dB/km), whereas the phase factor $\beta(\omega)$ (rad/m) exhibits dependence with respect to the frequency deviation and chromatic dispersion. The optical field signal is affected by the attenuation and the phase factors after propagates through an optical fiber with length L. In the model of optical fiber propagation characteristics, one should bear in mind the presence of some phenomena in the fiber channel, which are different in nature, occur simultaneously, and influence each other, namely: noise, filtering, nonlinear effects, and polarization mode dispersion. These effects impose limitations on the performance in modern optical transmission systems [9],[37]. This publication is concerned with the filtering phenomenon which stems from the fiber's chromatic dispersion, including waveguide and material [10].

All the optical signal spectral components will propagate through the optical fiber with different velocities, and the phase of each component will be changed by chromatic dispersion. The optical fiber phase factor could be expanded in a Taylor series around the carrier frequency ω_o. Taking into account the linear nature of the fiber and bearing in mind the spectral composition of the optical field at the output of the DD-MZM, the phase factor has optical spectral components with frequencies deviations equals to $\omega = \omega_o + n\omega_{RF}$. The interesting is on $\beta_2(\omega_o)$ coefficient related to the fiber chromatic dispersion parameter $D(\lambda)$, the optical carrier wavelength (λ_0), and the speed of light (c) in vacuum, according to [38]

$$\beta_2(\omega_o) = -\frac{D(\lambda)\lambda_0^2}{2\pi c} \tag{6}$$

The expression obtained for the output electrical field after propagation through a fiber with length L is given by

$$E_f(t) = 10^{\frac{-\alpha_{dB}L}{20}} \frac{E_o}{2} e^{j\omega_o t} \sum_{n=-\infty}^{+\infty} a_n e^{jn\omega_{RF}t} e^{j\frac{1}{2}(n\omega_{RF})^2 \beta_2(\omega_o)L} \tag{7}$$

At the output end of the SSMF, a square-law PD transforms the photon stream into an electric current. Introducing the concept of PD responsivity, it can be shown that the electrical photocurrent is proportional to the incident average optical power, hence it is also to the magnitude of the optical Poynting vector. By assuming a uniform power distribution over the fiber cross-section, the time dependent electric current is

$$i(t) = \Re \frac{E_f(t) E_f^*(t)}{2\xi} \tag{8}$$

where $\Re$ is the PD responsivity, ξ (Ω/m^2) is a constant that depends on both the fiber effective cross-section and the optical wave impedance, and $E_f(t)$ is the optical electrical field at the fiber link output according to Fig. 2(a). Equation (8) reveals that by applying the fiber output signal to the PD, beating signals between the optical spectral components will generate harmonics of the original radio-frequency (RF) modulating signal.

III. Frequency domain approach

In order to develop the frequency domain analysis, it might be possible to benefit from standard techniques developed for frequency domain analysis of a linear system [28],[39]. Once more, we remember the linear characteristics of the optical fiber and the propagation of the optical field along a linear standard single-mode fiber (SSMF). First, we took the Fourier's transform of (7) and we obtain the output electrical field in the frequency domain after propagation through a fiber with length L as

$$E_f(\omega, L) = 10^{\frac{-\alpha_{dB}L}{20}} \pi E_o \sum_{n=-\infty}^{+\infty} a_n \delta(\omega - n\omega_{RF}) e^{j\frac{1}{2}(n\omega_{RF})^2 \beta_2(\omega_o)L} \tag{9}$$

where δ represents the Dirac's delta function, and α is the fiber attenuation factor (dB/km). To detect the electric current at PD output, we must be able to use a model to predict dependence on frequency of such current. To this aim, we remember that the convolution theorem can be applied to rewrite the time domain expression of the PD current in the frequency domain as

$$I(\omega, L) = \Re \frac{E_f(\omega, L) * E_f^*(\omega, L)}{4\pi\xi} \tag{10}$$

Then, by applying the Graf's addition theorem for Bessel's functions [40], we obtained the expression for the detected electric current in the frequency domain, under the conditions that the modulation indexes are equal ($m_1 = m_2 = m$) and $n = N + k$ [41]:

$$\begin{aligned} I(N\omega_{RF}, L) = {} & 10^{\frac{-\alpha_{dB}L}{10}} \frac{\Re P_o}{4} \times \\ & \times (-1)^N \left\{ \left(e^{jN\theta_1} + 1\right) J_N\left[2m \sin\left(\frac{\phi}{2}\right)\right] + \right. \\ & + e^{jN\frac{\theta_1}{2}} \left\{ e^{j\theta_2} J_N\left[2m \sin\left(\frac{\phi + \theta_1}{2}\right)\right] + \right. \\ & \left. \left. + e^{-j\theta_2} J_N\left[2m \sin\left(\frac{\phi - \theta_1}{2}\right)\right]\right\}\right\} \end{aligned} \tag{11}$$

where

$$\phi = N\omega_{RF}^2 \beta_2(\omega_o) L \tag{12}$$

Equation (11) is an exact closed-form expression and was obtained without introducing any approximation, which also includes a few parameters such as the fiber attenuation and chromatic dispersion, PD responsivity, laser output power, and RF modulation index. The exact analytical formulation presented in this paper is in agreement with experimental results for ODSB push-pull and single-arm, and OSSB analog modulations formats, in which the expressions are in infinite series format [42].

Furthermore, (7) and (11) enables one to retrieve previous publications and it is in perfect agreement with many authors [27],[28]. The modeling of analog optical fiber link is synthesized by (11), it enables the frequency domain analysis of how the optical fiber chromatic dispersion affects the link performance which employs a nonlinear DD-MZM. The ϕ parameter given in (12) takes into account the RF harmonic order, chromatic dispersion, and fiber length.

The modulation index (m) is related to signal power and impedance of the RF source, and to the DD-MZM input impedance. The RF power delivered to the load is related to PD output impedance [43]. The link performance can be evaluated in terms of the RF output average power delivered to a load (R_L) as

$$P_{R_L}(N\omega_{RF}, L) = \frac{1}{2}\left|I(N\omega_{RF}, L)\right|^2 R_L \qquad (13)$$

IV. NUMERICAL RESULTS AND DISCUSSION

The numerical simulations were developed by using components with parameters specified in Table I. To validate our model, we developed our simulations with the same link parameters used in [28], and they were presented in [35].

Figure 5(a) shows the normalized RF fundamental power for 10GHz frequency in function of fiber length, for both exact and small-signal approaches, with ODSB modulation, $(\theta_1,\theta_2) = (\pi,\pi/2)$, and with modulation index (m) equal to 0.1. It is observed that by using small value for the modulation index, the two modeling are in agreement. The fiber length in which the RF power is minimum is about 36km, and it has a periodic variation as presented in [41]. However, if the modulation index increases, i.e., large-signal condition, the small-signal approximation moves away from the exact analysis, as Fig. 5(b). In this case, we use m = 1.916, related to the first root (3.832) of the J_1(.) Bessel function. New minimum points for the RF power will appear, in which the fiber length is about 0km and 73km. It can be seen that the increases in a RF power do not improve the link performance.

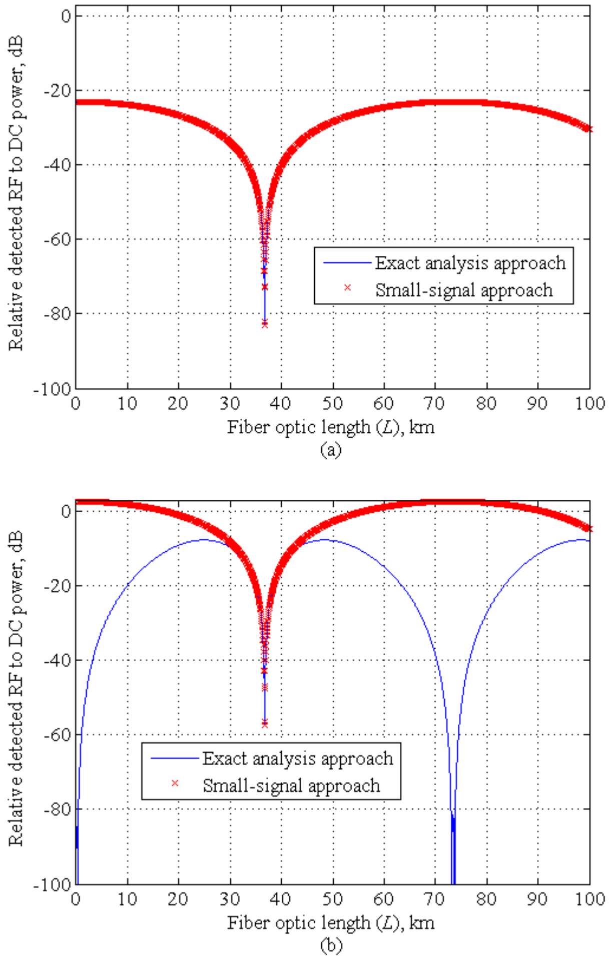

Fig. 5. Detected RF fundamental (N = 1) to DC power versus fiber length for the ODSB modulation $(\theta_1,\theta_2) = (\pi,\pi/2)$, where (a) uses a small modulation index value (m = 0.1), and (b) a large value (m = 1.916). The RF is 10GHz.

Figure 6(a) shows the normalized RF fundamental (10GHz) power in function of fiber length, for both exact and small-signal approaches, using the OSSB modulation, $(\theta_1,\theta_2) = (\pi/2,\pi/2)$, with m = 0.1. The link exhibits the special feature of RF fundamental power displaying very low sensitivity with respect to fiber chromatic dispersion. In this case, the two modeling are in agreement. However, if the modulation index is m = 1.916 (large-signal condition), a minimum point at about 36km for the detected RF power will appear, as in Fig. 6(b). This occurs because the ideal OSSB modulation is not achieved due to the influence of the others sidebands that compose the DD-MZM output spectrum (Fig. 4(b)).

TABLE I. TYPICAL VALUES OF PARAMETERS USED IN THE SIMULATION.

Parameter description	Symbol	Value
RF load impedance	Z_L	50Ω
Laser optical power	P_o	1mW
Laser wavelength	λ_0	1.55μm
SSMF attenuation [44]	α_{dB}	0.2dB/km
SSMF chromatic dispersion [44]	D	17ps/nm.km
Speed of light in vacuum	c	3x10^{8}m/s
PD responsivity [45]	$\Re$	0.75A/W

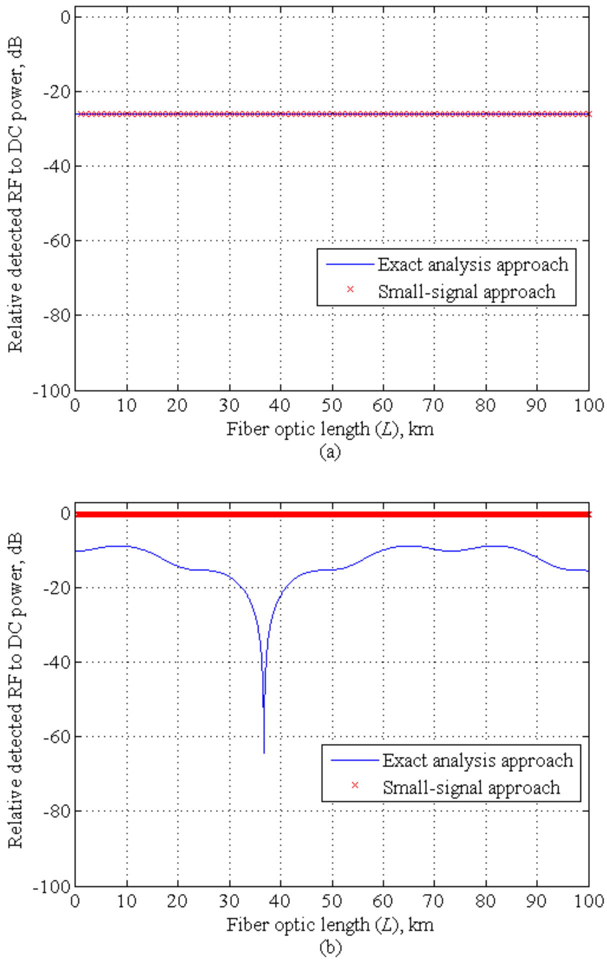

Fig. 6. Detected RF fundamental (N = 1) to DC power versus fiber length for the OSSB modulation $(\theta_1,\theta_2) = (\pi/2,\pi/2)$, where (a) uses a small modulation index value (m = 0.1), and (b) a large value (m = 1.916). The RF is 10GHz.

V. FINAL COMMENTS

This publication presented a very comprehensive frequency domain analytical model which enables the analysis of fiber chromatic dispersion effect and the influence of large modulation index in the performance of an IM-DD analog optical fiber link. The model besides relaying on parameters that suits experimental researchers, also allows one to retrieve important results widely available in literature, and will be very helpful for the system design. By using some optoelectronic components and devices, we performed numerical simulations that yielded results which seem to be of practical interest. The authors are working towards designing, implementing, and characterizing optical fiber link based on the model developed.

ACKNOWLEDGMENT

To the Electronic Warfare Laboratory at the Technological Institute of Aeronautics (ITA) and the National Institute of Telecommunications (INATEL).

REFERENCES

[1] J. Capmany, J. Mora, I. Gasulla, J. Sancho, J. Lloret, S. Sales, "Microwave Photonic Signal Processing," *Journal of Lightwave Technolgy*, vol. 31, no. 4, pp. 571-586, February 2013.

[2] J. Yao, "A tutorial on microwave photonics I," *IEEE Photonics Society Newsletter*, vol. 26, no. 2, pp. 4-12, April 2012.

[3] J. Yao, "A tutorial on microwave photonics II," *IEEE Photonics Society Newsletter*, vol. 26, no. 3, pp. 5-12, June 2012.

[4] A. J. Seeds, K. J. Williams, "Microwave Photonics," *Journal of Lightwave Technolgy*, vol. 24, no. 12, pp. 4628-4641, December 2006.

[5] A. J. Seeds, C.-P. Liu, T. Ismail, M. J. Fice, F. Pozzi, R. J. Steed, E. Rouvalis, C. C. Renaud, "Microwave Photonics," in *Conference on Lasers and Electro-Optics (CLEO) and Quantum Electronics and Laser Science Conference (QELS)*, pp. 1-2, May 2010.

[6] J. Capmany, B. Ortega, D. Pastor, "A Tutorial on Microwave Photonic Filters," *Journal of Lightwave Technology*, vol. 24, no. 1, pp. 201-229, January 2006.

[7] J. Martí, J. Capmany, "Microwave Photonics and Radio-over-Fiber Research," *IEEE Microwave Magazine*, vol. 10, no,4, pp. 96-105, June 2009.

[8] V. J. Urick, F. Bucholtz, J. D. McKinney, P. S. Devgan, A. L. Campillo, J. L. Dexter, K. J. Williams, "Long-Haul Analog Photonics," *Journal of Lightwave Technology*, vol. 29, no. 8, pp. 1182-1205, April 2011.

[9] R.-J. Essiambre, G. Kramer, P. J. Winzer, G. J. Foschini, B. Goebel, "Capacity Limits of Optical Fiber Networks," *Journal of Lightwave Technology*, vol. 28, no. 4, pp. 662-701, February 2010.

[10] P. J. Winzer, R.-J. Essiambre, "Advanced Optical Modulation Formats," *Proceedings of the IEEE*, vol. 94, no. 5, pp. 952-985, May 2006.

[11] P. J. Winzer, "Modulation and multiplexing in optical communication system," *IEEE LEOS News*, vol. 23, no. 1, pp. 4-10, February 2009.

[12] H. Zhang, S. Pan, M. Huang, X. Chen, "Polarization-modulated analog photonic link with compensation of the dispersion-induced power fading," *Optics Letters*, vol. 37, no. 5, pp. 866-868, March 2012.

[13] S. Li, X. Zheng, H. Zhang, B. Zhou, "Compensation of dispersion-induced power fading for highly linear radio-over-fiber link using carrier phase-shifted double sideband modulation," *Optics Letters*, vol. 36, no. 4, pp. 546-548, February 2011.

[14] G. Zhang, X. Zheng, S. Li, H. Zhang, B. Zhou, "Postcompensation for nonlinearity of Mach–Zehnder modulator in radio-over-fiber system based on second-order optical sideband processing," *Optics Letters*, vol. 37, no. 5, pp. 806-808, March 2012.

[15] B. Vidal, "Analytical model for hybrid amplitude and phase modulation in dispersive radio over fiber links," *Optics Communications*, vol. 284, no. 21, pp. 5138-5143, October 2011.

[16] B. Hraimel, X. Zhang, Y. Pei, K. Wu, T. Liu, T. Xu, Q. Nie, "Optical Single-Sideband Modulation With Tunable Optical Carrier to Sideband Ratio in Radio Over Fiber Systems," *Journal of Lightwave Technology*, vol. 29, no. 5, pp. 775-781, March 2011.

[17] P.-Y. Wu, H.-H. Lu, C.-L. Ying, C.-Y. Li, H.-S. Su, "An Upconverted Phase-Modulated Fiber Optical CATV Transport System," *Journal of Lightwave Technology*, vol. 29, no. 16, pp. 2422-2427, August 2011.

[18] C. Lim, A. Nirmalathas, M. Bakaul, P. Gamage, K.-L. Lee, Y. Yang, D. Novak, R. Waterhouse, "Fiber-Wireless Networks and Subsystem Technologies," *Journal of Lightwave Technology*, vol. 28, no. 4, pp. 390-405, February 2010.

[19] J. Yao, "Microwave Photonics," in *IEEE International Workshop on Electromagnetics, Applications and Student Innovation (iWEM), 2012*, pp. 1-2, August 2012.

[20] A. A. Ferreira Júnior, O. L. Coutinho, C. S. Martins, J. A. J. Ribeiro, V. R. Almeida, J. E. B. Oliveira, "Analytical modelo f optical fiber chromatic dispersion effect in upconverted millimeter-wave long-haul fiber optic link," in *International Workshop on Telecommunications (IWT)*, pp. 1-8, May 2013.

[21] S. Zhang, R. Lu, D. Chen, S. Liu, Y. Liu, "High-frequency characterization of an optical phase modulator with phase modulation-to-intensity modulation conversion in dispersive fiber," *Chinese Science Bulletin*, vol. 57, no. 22, pp. 2929-2933, August 2012.

[22] M. Wang, J. Yao, "Optical vector network analyzer based on unbalanced double-sideband modulation," *IEEE Photonics Technology Letters*, vol. 25, no. 8, pp. 753-756, April 2013.

[23] Z. Tang, S. Pan, J. Yao, "A high resolution optical vector network analyzer based on a wideband and wavelength-tunable optical single-sideband modulator," *Optics Express*, vol. 20, no. 6, pp. 6555-6560, March 2012.

[24] J. Li, X. Zhang, B. Hraimel, T. Ning, L. Pei, K. Wu, "Performance analysis of photonic-assisted periodic triangular-shaped pulses generator," *Journal of Lightwave Technology*, vol. 30, no. 11, pp. 1617-1624, June 2012.

[25] S. Iezekiel, "Measurements of Microwave Behavior in Optical Links," *IEEE Microwave Magazine*, vol. 9, no. 3, pp. 100-120, June 2008.

[26] C. Lim, A. Nirmalathas, M. Bakaul, K.-L. Lee, D. Novak, R. Waterhouse, "Mitigation strategy for transmission impairments in millimeter-wave radio-over-fiber networks," *Journal of Optical Networking*, vol. 8, no. 2, pp. 201-214, February 2009.

[27] J. L. Corral, J. Marti, J. M. Fuster, "General expressions for IM/DD dispersive analog optical links with external modulation or optical up-conversion in Mach–Zehnder electrooptical modulator," *IEEE Transactions on Microwave Theory and Techniques*, vol. 49, no. 10, pp. 1968-1976, October 2001.

[28] L. Cheng, S. Aditya, A. Nirmalathas, "An Exact Analytical Model for Dispersive Transmission in Microwave Fiber-Optic Links Using Mach-Zehnder External Modulator," *IEEE Photonics Technology Letters*, vol. 17, no. 7, pp. 1525-1527, July 2005.

[29] A. Yariv, P. Yeh, P, "Photonics: Optical Electronics in Modern Communications," 6th edition, Oxford University Press: New York, 2007.

[30] C.-T. Lin, J. Chen, S.-P. Dai, P.-C. Peng, S. Chi, "Impact of Nonlinear Transfer Function and Imperfect Splitting Ratio of MZM on Optical Up-Conversion Employing Double Sideband With Carrier Suppression Modulation," *Journal of Lightwave Technology*, vol. 26, no. 15, pp. 2449-2459, August 2008.

[31] Morant, R. Llorente, J. Hauden, T. Quinlan, A. Mottet, S. Walker, "Dual-drive $LiNbO_3$ interferometric Mach-Zehnder architecture with extended linear regime for high peak-to-average OFDM-based communication systems," *Optics Express*, vol. 19, no. 26, pp. B450-B456, December 2011.

[32] D. Janner, D. Tulli, M. Belmonte, V. Pruneri, "Waveguide electro-optic modulation in micro-engineered $LiNbO_3$," *Journal of Optics A: Pure and Applied Optics*, no. 10, pp. 1-6, 2008.

[33] C. Kitano, J. E. B. Oliveira, "Dispositivos à Óptica Integrada para Aplicações em Telecomunicações," *Revista Telecomunicações*, vol. 3, no. 2, pp. 27-38, Dezembro 2000.

[34] J. E. B. Oliveira, J. A. J. Ribeiro, "Interfaces para Enlaces de Fibra Óptica de Alta Velocidade," *Revista Telecomunicações*, vol. 3, no. 2, pp. 65-75, Dezembro 2000.

[35] A. A. Ferreira Júnior, O. L. Coutinho, C. S. Martins, W. S. Fegadolli, J. A. J. Ribeiro, J. E. B. Oliveira, "Effect of Fiber Optic Chromatic Dispersion on the Performance of Analog Optical Link with Dual-Drive Mach-Zehnder Modulator," in *Simpósio de Aplicações Operacionais em Área de Defesa (XIV SIGE)*, pp. 119-126, 2012.

[36] M. Xue, Y. Zhao, X. Gu, S. Pan, "Performance analysis of optical vector networks analyzer based on optical single-sideband modulation," *Journal of Optical Society of America B*, vol. 30, no. 4, pp. 928-933, April 2013.

[37] L. G.-Nielsen, M. Wandel, P. Kristensen, C. Jorgensen, L. V. Jorgensen, B. Edvold, B. Pálsdóttir, D. Jakobsen, "Dispersion-Compensating Fibers," *Journal of Lightwave Technology*, vol. 23, no. 11, pp. 3566-3579, November 2005.

[38] G. P. Agrawal, "Fiber-Optic Communication Systems," 3rd edition, John Wiley & Sons: New York, 2002.

[39] E. Vos, "Frequency Domain Approach for Optimizing Optical Frequency Multiplication System using Mach-Zehnder- and Fabry-Perot- Interferometer," in *Graduation Symposium – Eindhoven University of Technology*, pp. 1-12, August 2008.

[40] M. Abramowitz, I. Stegun, "Handbook of Mathematical Functions with Formulas, Graphs, and Mathematical Tables," Dover Publications: New York, 1965.

[41] A. A. Ferreira Jr., O. L. Coutinho, C. S. Martins, W. S. Fegadolli, J. A. J. Ribeiro, V. R. Almeida, J. E. B. Oliveira, "Effect of Fiber Optic Chromatic Dispersion on the Performance of Analog Optical Link with External Modulation Aiming at Aerospace Applications," *Journal of Aerospace Technology and Management*, vol. 5, no. 2, pp. 205-216, April-June 2013.

[42] J. Han, B.-J. Seo, Y. Han, B. Jalali, H. R. Fetterman, "Reduction of fiber chromatic dispersion effects in fiber-wireless and photonic time-stretching system using polymer modulators," *Journal of Lightwave Technology*, vol. 21, no. 6, pp. 1504-1509, June 2003.

[43] O. L. Coutinho, V. R. Almeida, J. E. B. Oliveira, "Analysis of analog fiber optical links based on DSB+C and SSB+C modulation techniques," in *International Conference on Microwave and Optoelectronics (SBMO/IEEE MTT-S)*, pp. 439-443, July 2005.

[44] Corning® SMF-28® Optical Fiber Product Information. From: http://www.corning.com/WorkArea/showcontent.aspx?id=41261. Access: June 25, 2013.

[45] ThorLabs DET10D. From: http://www.thorlabs.com/Thorcat/13100/DET10D-Manual.pdf. Access: June 25, 2013.